保偏铒镱共掺光纤制备及其激光性能研究

李文臻[1]，陈阳[1]，廖雷[2]，褚应波[1]，戴能利[1]，李进延[1*]

[1]华中科技大学武汉光电国家研究中心，湖北 武汉 430074；
[2]武汉长进激光技术有限公司，湖北 武汉 430223

摘要　随着激光雷达技术的快速发展，激光雷达在军事及民用领域中的应用不断增多。保偏铒镱共掺光纤是 1.5 μm 激光雷达重要的增益介质，对其性能有重要的影响。成功制备出 10 μm/128 μm 保偏铒镱共掺光纤，其双折射系数为 1.29×10^{-4}，在 1310 nm 处的消光比为 24 dB@4 m。基于该光纤搭建了全保偏全光纤主振荡功率放大系统，实验结果显示，当信号波长为 1551 nm，光纤长度为 7.5 m，940 nm 泵浦功率为 16.5 W 时，输出功率为 5.8 W，斜率效率达 36%，输出激光的消光比为 21 dB。该保偏铒镱共掺光纤具有优异的激光性能，为 1.5 μm 激光雷达系统的国产化提供了新的解决方案。

关键词　光纤光学；光纤激光器；铒镱共掺；激光雷达；保偏光纤

中图分类号　O436　　　**文献标志码**　A　　　　　　　　　　　　　　**DOI**：10.3788/CJL202249.1206006

1　引　言

激光雷达被广泛应用于测距测风、无人驾驶和遥感测绘等领域。激光光源发出的激光脉冲在到达物体表面后发生反射，反射后的光信号被接收机探测并被转换成电信号，经算法分析可得到物体的方位、姿态和距离等信息[1]。对于激光雷达系统而言，激光光源是影响整个系统性能的至关重要的因素[2]。光纤激光器由于其高光束质量、高脉冲能量和高重复频率等特点[3-5]，已经成为激光雷达用光源的最佳选择。其中，相比现有的 1 μm 掺镱光纤激光，保偏（PM）铒镱共掺光纤产生的 1550 nm 激光由于具有"人眼安全"、大气传输损耗低等特点[6-7]，吸引了研究者的广泛关注[8-11]。2021 年，Booker 等[12]为了研究引力波探测所用的相干光源，采用 Nufern 公司生产的 PLMA-EYDF-25P/300-HE 保偏铒镱共掺光纤，搭建了二级单频光纤放大系统，系统中未观察到受激布里渊散射（SBS）现象，最终激光输出功率为 110 W，信噪比大于 50 dB。2020 年，Wei 等[13]采用 CorActive 公司生产的 DCF-EY-10/128-PM 保偏铒镱共掺光纤，搭建了带有双波长辅助信号的窄线宽铒镱共掺光纤放大器，实现的输出功率为 13.8 W，线宽为 3.5 kHz。2018 年，Lee 等[14]搭建了三级全保偏光纤单频主振荡功率放大（MOPA）光脉冲系统，在 1572 nm 处实现了单脉冲能量为 1.8 mJ、峰值功率为 3.5 kW、重复频率为 2.5 kHz 的脉冲激光。然而，以上研究所用的光纤均为国外公司生产。在国内，由于保偏铒镱共掺光纤的制备相对困难，仅 2015 年中国电子科技集团公司第四十六研究所报道过保偏铒镱共掺光纤的制备[15]，但基于该保偏铒镱共掺光纤的激光性能研究未曾报道，国产光纤在 1550 nm 激光雷达领域中的应用仍有待突破。

保偏铒镱共掺光纤作为激光雷达用光纤激光器的最重要增益介质[16-18]，具有重要的研究意义。本文基于改进化学气相沉积（MCVD）法[19]，结合液相掺杂工艺（SDT），通过高精度打孔技术成功制备出保偏铒镱共掺光纤，并测试了光纤结构参数及光学性能。结果显示，其双折射系数（B 值）为 1.29×10^{-4}，在 1310 nm 处的消光比为 24 dB@4 m。为进一步研究基于该保偏铒镱共掺光纤的激光性能，搭建了基于全光纤主振荡功率放大结构的保偏测试平台，实现了功

率为 5.8 W 的激光输出,斜率效率达到 36％。

2　光纤制备与表征

高掺 P_2O_5 能够促进 Yb^{3+} 向 Er^{3+} 的能量传递,提升 Er^{3+} 发光效率,是制备保偏铒镱共掺光纤的关键。然而,常规 MCVD 制备工艺很难实现高 P_2O_5 含量掺杂,进而无法实现铒镱共掺光纤的高效率输出。本文通过 MCVD 工艺,结合 SDT 制备了铒镱共掺光纤预制棒,并结合反向掺磷及气相补偿,将纤芯 P_2O_5 含量(摩尔分数)提高到 10％以上。

按光纤尺寸对所制备的铒镱共掺光纤预制棒进行套管处理,然后在预制棒纤芯两侧打孔,并插入合适尺寸的硼棒以形成熊猫眼型保偏光纤预制棒,最后通过拉丝塔拉制出 10 μm/128 μm 保偏铒镱共掺光纤。由于预制棒纤芯应力较大,为了避免打孔时纤芯炸裂产生缺陷,需先将光纤预制棒放于退火炉中,在 670～690 ℃温度下放置 72 h 进行退火处理,然后将温度逐渐恢复至室温,以释放纤芯内的残余应力。其中,打孔制备保偏铒镱共掺光纤预制棒的流程如图 1 所示,为了提高光纤的双折射性能,尽量选取靠近纤芯的位置进行打孔,并采用高浓度硼棒进行加工。通过电子探针显微分析仪(EPMA),在光纤
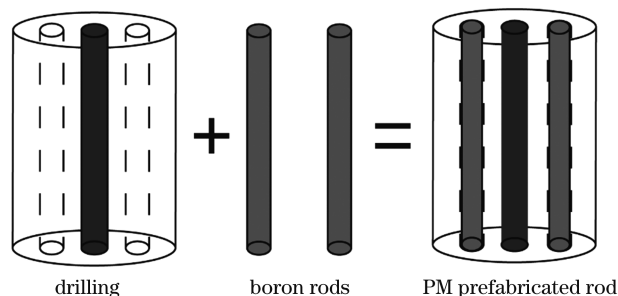

图 1　打孔制备保偏铒镱共掺光纤预制棒的流程

Fig. 1　Drilling fabrication process of prefabricated rod of polarization maintaining erbium-ytterbium co-doped fiber

表面探测纤芯元素含量及硼棒浓度,其 Er、Yb、P 离子的归一化浓度(质量分数)如图 2(a)所示。高掺磷使得光纤能够更好地抑制 Er^{3+} 向 Yb^{3+} 的反向能量传递,减少 1 μm 放大自发辐射(ASE)的产生,检测到的硼浓度(摩尔分数)为 25.9％。光纤截面如图 2(b)插图所示,其纤芯直径为 10.19 μm,包层直径为 128.69 μm,硼棒直径为 32.59 μm,纤芯与硼棒的间距为 13.00 μm。预制棒的折射率剖面如图 2(b)所示,纤芯的数值孔径为 0.24,计算分析结果显示,拉制光纤支持的纤芯模式有 LP01、LP02、LP11、LP21 和 LP31。此外,通过截断法测量了 940 nm 处的包层吸收,吸收系数约为 2.42 dB/m。
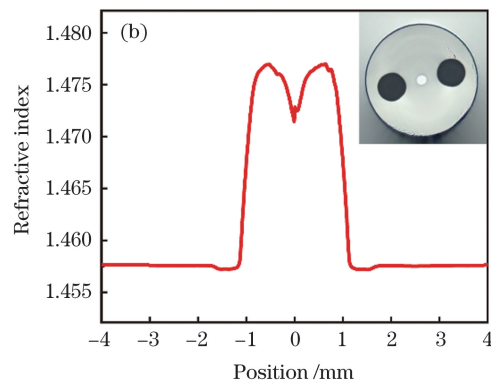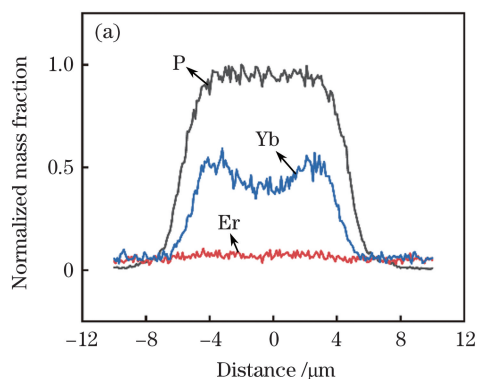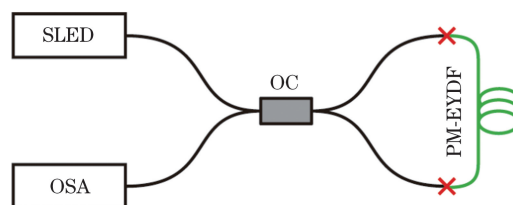

图 2　光纤及预制棒的表征。(a) 光纤的径向掺杂浓度;(b) 预制棒纤芯的折射率剖面,插图为光纤截面

Fig. 2　Characterizations of fiber and prefabricated rod. (a) Radial doping concentration of fiber; (b) refractive index profile of prefabricated rod core with cross-section of optical fiber shown in insert

基于 Sagnac 干涉环对保偏光纤进行拍长测量,进而求出其双折射系数,测量结构如图 3 所示。该结构采用的宽谱光源波长范围为 1250～1650 nm,光谱分析仪为横河公司生产的 AQ6370D,其中光源和光谱仪与待测光纤分别接在 3 dB 耦合器(OC)两端,待测光纤为长度为 50 cm 的自制的 10 μm/128 μm 保偏铒镱共掺光纤。由于计算的是 1550 nm 处的双折射系数,因此在光谱仪中观察 1500～1600 nm 处的干涉图像,其干涉图像如图4所示。通过计算

SLED: superluminescent diode; OC: optical coupler;
OSA: optical spectrum analyzer

图 3　测量拍长的 Sagnac 干涉环的结构图

Fig. 3　Structural diagram of Sagnac interference ring for measuring beat length
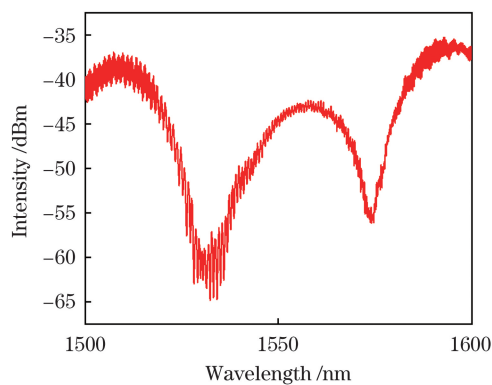
图 4 待测光纤的干涉图像

Fig. 4　Interference image of test fiber

可知，光纤在 1550 nm 处的拍长为 9 mm，所对应的双折射系数为 1.29×10^{-4}。

采用 1310 nm 保偏光源测量消光比，光源输出的原始种子光的功率为 10 dBm，消光比测试仪测出的消光比为 29 dB。通过一段 4 m 长的自研保偏铒镱共掺光纤后，消光比测量结果为 24 dB，测试结构如图 5 所示。
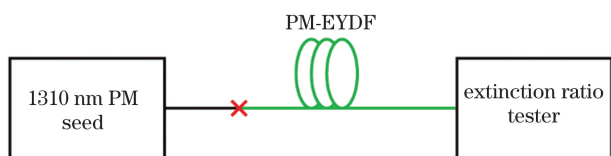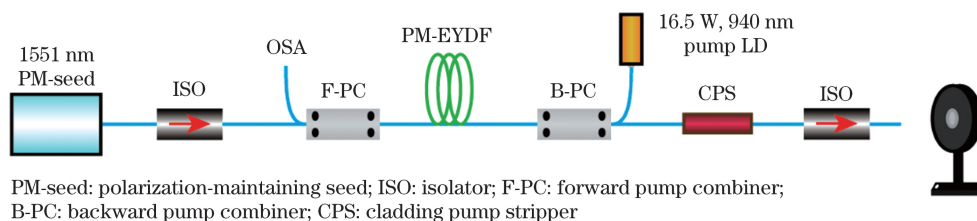
图 5 消光比测试结构

Fig. 5　Test structure for extinction ratio

3　激光实验装置

保偏铒镱共掺光纤的实验装置如图 6 所示，种子源设置功率为 20 mW、中心波长为 1551 nm，接在光源后的隔离器（ISO）用于保护种子源。隔离器采用双轴工作模式，在隔离器后面接一个（2+1）×1 的前向泵浦合束器（PC），通过其泵浦臂监测回光功率，同时观察后向光谱。输出端熔接自研的 10 μm/128 μm 保偏铒镱共掺光纤，长度分别取为 8.0，7.5，7.0，6.5 m，光纤的弯曲直径保持在 10 cm。由半导体激光器（LD）产生的 940 nm 泵浦光经（2+1）×1 反向 PC 的泵浦臂耦合进有源光纤，泵浦注入功率为 16.5 W。通过在反向 PC 输出端涂覆高折射率胶制备包层光剥除器（CPS），用于滤除光纤中的包层光，提高激光输出质量。在激光输出端前放置 ISO 以防止端面反射产生的回返光损坏器件并抑制 ASE 在回路中来回振荡产生寄生激光。实验中其余光纤均悬空并切 8°斜角，有源光纤采用风冷进行散热。

4　实验结果与讨论

中心波长为 1551 nm 的保偏种子源功率设置为 20 mW，由于 ISO 和（2+1）×1 前向 PC 的固有损耗，最终耦合进入有源光纤的种子光功率为 17.5 mW。当泵浦功率为 16.5 W，有源光纤长度为 7.5 m 时，斜率效率达到最大，约为 36%，其输出的信号光功率为 5.8 W，消光比为 21 dB。图7（a）显示了不同

PM-seed: polarization-maintaining seed; ISO: isolator; F-PC: forward pump combiner;
B-PC: backward pump combiner; CPS: cladding pump stripper

图 6 MOPA 全光纤激光器的结构图

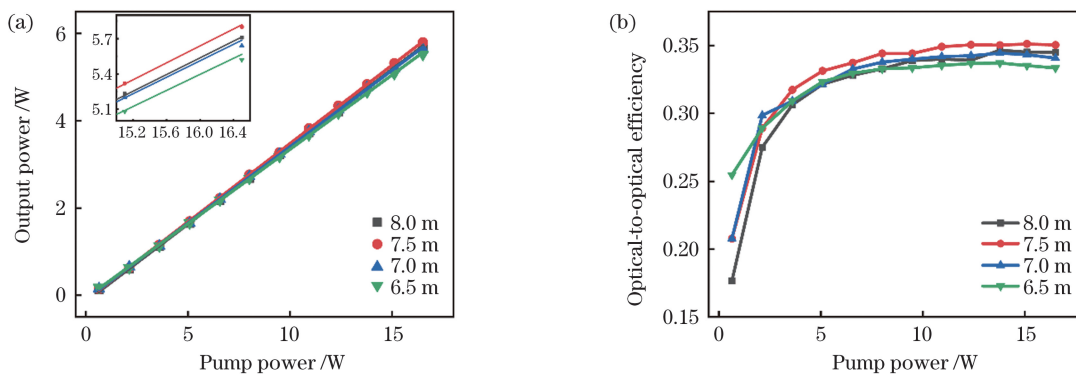Fig. 6　Structural diagram of MOPA all-fiber laser

图 7 不同光纤长度下的效率。（a）斜率效率；（b）光光效率

Fig. 7　Efficiencies under different fiber lengths. (a) Slope efficiency; (b) optical-to-optical efficiency

光纤长度下的斜率效率情况。此外，如图 7(b)所示，当光纤长度为 6.5，7.0，7.5，8.0 m 时，光光效率均大于 33%，且无下降趋势，说明此时激光功率可进一步增加。

当纤长优化至 7.5 m 时，系统的前后向光谱如图 8 所示。图 8(a)插图为系统的输出窄谱，随着泵浦功率的增加，放大自发辐射的功率逐渐变大，但信噪比仍维持在 50 dB 以上。输出光谱上出现规律的干涉峰，这是由种子源的输出特性导致的。最大泵浦功率时的输出光谱如图 8(a)所示，光谱中并未观

察到剩余泵浦光和 1 μm ASE 的出现，说明该光纤可较好抑制 1 μm ASE。从图 8(b)中后向光谱可以观察到，剩余泵浦光的强度稳定，这可能是由于此时保偏光纤中存在一定的未被纤芯吸收的螺旋泵浦光且未加 CPS 滤模。另一方面，随着泵浦功率的增加，后向 1 μm ASE 开始逐步增强，当泵浦功率超过 10 W 后，1064 nm 处的 ASE 相对于其他波长处的 ASE 急剧增强，但并未生成寄生振荡。由此可知，本文制备的保偏铒镱共掺光纤具有良好的激光性能。
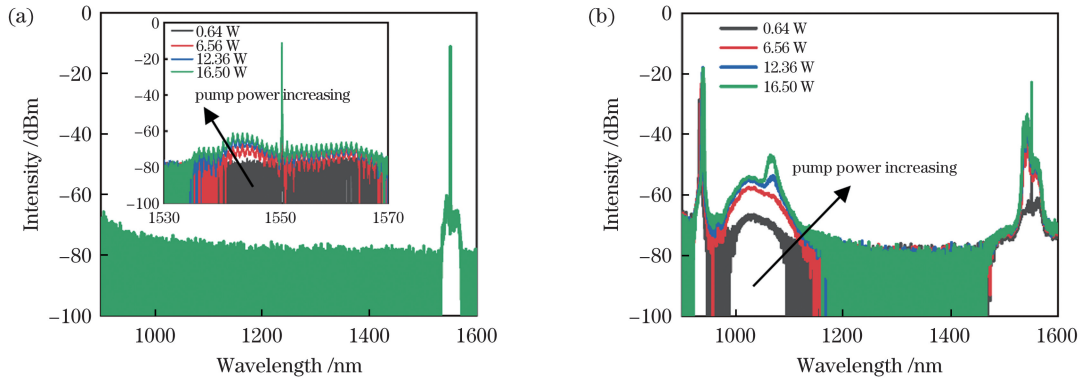

图 8　不同泵浦功率下的光谱。(a) 输出光谱，插图为不同泵浦功率下的窄谱；(b) 后向光谱

Fig. 8　Spectra at different pump powers. (a) Output spectrum with narrow spectra at different pump powers shown in inset；(b) backward spectra

5　结　　论

采用 MCVD 技术结合 SDT 成功制备了激光雷达用保偏铒镱共掺光纤。测试了保偏光纤的双折射性能，其双折射系数为 $1.29×10^{-4}$，在 1310 nm 处的消光比为 24 dB@4 m。实验进一步搭建了基于全保偏全光纤铒镱共掺光纤的激光测试系统，测得斜率效率达到 36%。实现了国产保偏铒镱共掺光纤的最高效率，为激光雷达的国产化提供了可能。

参 考 文 献

[1] 刘菲菲, 毕德仓, 刘恒, 等. 临近空间激光测风雷达原理样机和实验进展[J]. 中国激光, 2020, 47(8): 0810003.
　　Liu F F, Bi D C, Liu H, et al. Principle prototype and experimental progress of wind lidar in near space [J]. Chinese Journal of Lasers, 2020, 47(8): 0810003.

[2] 史伟, 房强, 李锦辉, 等. 激光雷达用高性能光纤激光器[J]. 红外与激光工程, 2017, 46(8): 0802001.
　　Shi W, Fang Q, Li J H, et al. High-performance fiber lasers for LIDARs [J]. Infrared and Laser Engineering, 2017, 46(8): 0802001.

[3] Gao C X, Zhu S L, Zhao W, et al. Eye-safe, high-energy, single-mode all-fiber laser with widely tunable repetition rate[J]. Chinese Optics Letters, 2009, 7(7): 611-613.

[4] Wu T Y, Dou Z Y, Zhang B, et al. Noise-like rectangular pulses in a mode-locked double-clad Er:Yb laser with a record pulse energy[J]. Chinese Physics B, 2020, 29(1): 014202.

[5] Holmen L G, Rustad G, Haakestad M W. Eye-safe fiber laser for long-range 3D imaging applications[J]. Applied Optics, 2018, 57(23): 6760-6767.

[6] Zhang J, Fromzel V, Dubinskii M. Resonantly cladding-pumped Yb-free Er-doped LMA fiber laser with record high power and efficiency[J]. Optics Express, 2011, 19(6): 5574-5578.

[7] Supradeepa V R, Nicholson J W. Power scaling of high-efficiency 1.5 μm cascaded Raman fiber lasers [J]. Optics Letters, 2013, 38(14): 2538-2541.

[8] 温强, 王超梅, 李尧, 等. 基于 MOPA 结构的 1550 nm 单频脉冲光纤激光器[J]. 激光与红外, 2020, 50(8): 948-952.
　　Wen Q, Wang C M, Li Y, et al. 1055 nm single-frequency pulsed fiber laser based on MOPA structure[J]. Laser & Infrared, 2020, 50(8): 948-952.

［9］ Pavlov I, Dülgergil E, Ilbey E, et al. Diffraction-limited, 10-W, 5-ns, 100-kHz, all-fiber laser at 1.55 μm[J]. Optics Letters, 2014, 39(9): 2695-2698.

［10］ Kuhn V, Wessels P, Neumann J, et al. Stabilization and power scaling of cladding pumped Er:Yb-codoped fiber amplifier via auxiliary signal at 1064 nm[J]. Optics Express, 2009, 17(20): 18304-18311.

［11］ 王筱晔, 吴松华, 刘晓英, 等. 基于相干多普勒激光雷达的飞机尾涡观测[J]. 光学学报, 2021, 41(9): 0901001.
Wang X Y, Wu S H, Liu X Y, et al. Observation of aircraft wake vortex based on coherent Doppler lidar [J]. Acta Optica Sinica, 2021, 41(9): 0901001.

［12］ Booker P, de Varona O, Steinke M, et al. Two-stage fully monolithic single-frequency Er:Yb fiber amplifier at 1556 nm for next-generation of gravitational wave detectors [J]. Proceedings of SPIE, 2021, 11665: 1116650O.

［13］ Wei S S, Yao B, Chen Y J, et al. Cladding-pumped erbium-ytterbium co-doped fiber amplifier with dual-wavelength auxiliary signal injection of 1030 nm and 1040 nm[J]. IEEE Photonics Journal, 2020, 12(2): 19447759.

［14］ Lee W, Geng J H, Jiang S B, et al. 1.8 mJ, 3.5 kW single-frequency optical pulses at 1572 nm generated from an all-fiber MOPA system[J]. Optics Letters, 2018, 43(10): 2264-2267.

［15］ 耿鹏程, 衣永青, 潘蓉, 等. 高吸收系数铒镱共掺保偏光纤的制备[J]. 光纤与电缆及其应用技术, 2015 (5): 26-28.
Geng P C, Yi Y Q, Pan R, et al. Preparation of Er^{3+}-Yb^{3+} co-doped polarization maintaining fiber with high absorption coefficient[J]. Optical Fiber & Electric Cable and Their Applications, 2015(5): 26-28.

［16］ Yang C S, Xu S H, Mo S P, et al. 10.9 W kHz-linewidth one-stage all-fiber linearly-polarized MOPA laser at 1560 nm[J]. Optics Express, 2013, 21(10): 12546-12551.

［17］ Zhao Z G, Xuan H W, Igarashi H, et al. Single frequency, 5 ns, 200 μJ, 1553 nm fiber laser using silica based Er-doped fiber [J]. Optics Express, 2015, 23(23): 29764-29771.

［18］ Liu Y, Liu J Q, Chen W B. Eye-safe, single-frequency pulsed all-fiber laser for Doppler wind lidar [J]. Chinese Optics Letters, 2011, 9(9): 090604.

［19］ Khudyakov M M, Lobanov A S, Lipatov D S, et al. Single-mode large-mode-area Er-Yb fibers with core based on phosphorosilicate glass highly doped with fluorine[J]. Laser Physics Letters, 2019, 16(2): 025105.

Fabrication and Laser Performance of Polarization-Maintaining Erbium-Ytterbium Co-Doped Fiber

Li Wenzhen[1], Chen Yang[1], Liao Lei[2], Chu Yingbo[1], Dai Nengli[1], Li Jinyan[1*]

[1] *Wuhan National Laboratory for Optoelectronics, Huazhong University of Science and Technology, Wuhan 430074, Hubei, China*;

[2] *Wuhan Changjin Laser Technology Co., Ltd., Wuhan 430223, Hubei, China*

Abstract

Objective　Lidar has been widely used in wind ranging, automatic drive and sensing mapping. The reflected light signal is obtained through first emitting a Gaussian beam from the laser source and then reflecting after reaching the surface of the object. After the computer analysis, the information of the object such as orientation, attitude and distance can be obtained. However, as for a lidar system, its laser source is an important unit influencing the performance of the whole system. A fiber laser has become the best choice of the light source for a lidar system, because of its good beam quality, high pulse energy and high repetition rate. At the same time, an erbium-ytterbium co-doped fiber has attracted the attention of many researches due to its advantages such as "eye-safe" and low atmospheric transmission loss. Therefore, as the most important gain medium for the laser lidar, polarization-maintaining erbium-ytterbium co-doped fiber has important research significance. In this paper, a 10 μm/128 μm polarization-maintaining erbium-ytterbium co-doped fiber is successfully fabricated by the modified chemical vapor deposition (MCVD) technique combined with the solution doping technology (SDT). The structural parameters and optical properties of this polarization-maintaining erbium-ytterbium co-doped fiber are measured. And its laser

performance is also studied.

Methods MCVD combined with SDT is used to fabricate the erbium-ytterbium co-doped fiber. The content (mole fraction) of P_2O_5 in the core is increased by more than 10% with reverse phosphorus doping and gas phase compensation. In order to avoid the defect of the core bursting during drilling, the fiber prefabricated rod is first annealed due to the high stress of its core. Through the Sagnac interferometer and the optical spectrum analyzer (OSA), the birefringence value is measured. The measurement structure is shown in Fig. 3. And the measurement structure of polarization extinction ratio is also shown in Fig. 5. In order to analyze the laser performance, the structure of an erbium-ytterbium co-doped fiber laser is shown in Fig. 6. The seed source has a power of 20 mW and a central wavelength of 1551 nm. An isolator (ISO) connected to the seed is used to protect the seed source. The isolator is followed by a $(2+1)\times1$ forward pump combiner (PC), and one of its pump fiber is used to monitor the backward power and observe the backward spectrum. The 940 nm light generated by the laser diode (LD) is coupled to the active fiber through the pump fiber of the $(2+1)\times1$ backward PC, and the pump power is 16.5 W. The coiling diameter of the active fiber is 10 cm. The cladding pump stripper (CPS) is implemented by coating a high refractive index adhesive to filter cladding light from the fiber. Finally, an isolator is fused at the end to prevent reflection.

Results and Discussions The dimension of the fiber is shown in the inset of Fig. 2(b). The diameters of core and cladding are measured to be 10.19 μm and 128.69 μm, respectively. The diameter of the boron rod is measured to be 32.59 μm. Figure 2(b) shows the refractive index profile of the prefabricated rod. A numerical aperture of 0.24 is finally achieved. The absorption coefficient measured by the truncation method is 2.42 dB/m at 940 nm. The interference image at 1500–1600 nm is observed in the OSA (Fig. 4). The beat length at 1550 nm is calculated to be 9 mm with a birefringence coefficient of 1.29×10^{-4}. At the same time, a polarization extinction ratio of 24 dB at 1310 nm is measured through the erbium-ytterbium co-doped fiber with a length of 4 m. As for the laser performance, due to the inherent loss, the final seed power coupling into the active fiber is 17.5 mW. Figure 7(a) shows the slope efficiency under different fiber lengths and pump powers. It can be seen from this figure that the optimal length is 7.5 m. When the pump power is 16.5 W, the output power and the slope efficiency reach the maximum, which are 5.8 W and 36%, respectively. The polarization extinction ratio is measured to be 21 dB. In addition, as shown in Fig. 7(b), the optical-to-optical efficiency tends to be saturated with the increase of pump power at different lengths. After reaching the saturation state, the optical-to-optical efficiency is more than 33% without a downward trend, which indicates that the laser power can be further increased at this time. The spectrum at 7.5 m is shown in Fig. 8. It can be observed from this output spectrum that the amplified spontaneous emission (ASE) power increases gradually with the increase of pump power, but the signal-to-noise ratio remains above 50 dB. From the backward spectrum, one can observe that the remaining pump light intensity is stable, which may be caused by the fact that some spiral pump light in the polarization-maintaining fiber is not absorbed by the fiber and the CPS is not added. Meanwhile, there is no parasitic oscillation at 1 μm. It shows that the polarization-maintaining erbium-ytterbium co-doped fiber prepared in this paper has good laser performances.

Conclusions In this paper, a polarization-maintaining erbium-ytterbium co-doped fiber for lidar is successfully fabricated by MCVD combined with SDT. The performance of this polarization-maintaining fiber is measured. A birefringence coefficient of 1.29×10^{-4} and a polarization extinction ratio of 24 dB@4 m at 1310 nm are achieved. In addition, a polarization-maintaining all-fiber erbium-ytterbium co-doped fiber laser system is built, and the slope efficiency reaches 36%. Above all, the highest efficiency of the polarization-maintaining erbium-ytterbium co-doped fiber is achieved, which provides the possibility for exact localization of a military lidar.

Key words fiber optics; fiber lasers; erbium-ytterbium co-doping; lidar; polarization-maintaining fiber